Cureus Journal of Computer Science

Open Access Original Article

Timely Detection of Lung Nodule Malignancy Using 3D Convolutional Neural Networks

Lakshmi E. Chetan [1] , Sivva Abhinay [2] , Chikatimalla Akshay Sri Ranga [2] , Madhusudhana E. Reddy [3] , Naga A. Malleswara Rao [3]

1. Department of Computer and Communication Engineering, Amrita Vishwa Vidyapeetham, Hyderabad, IND 2. Department of Computer Science and Engineering, Amrita Vishwa Vidyapeetham, Hyderabad, IND 3. Department of Computer Science and Engineering, Sree Dattha Institute of Engineering and Science, Hyderabad, IND

Corresponding authors: Lakshmi E. Chetan, echetan246@gmail.com, Madhusudhana E. Reddy, e_mreddy@yahoo.com

Received 06/05/2025
Review began 06/10/2025
Review ended 07/11/2025
Published 07/14/2025

DOI: https://doi.org/10.7759/s44389-025-06619-1

Abstract

Lung cancer remains one of the leading causes of cancer death worldwide, with most cases diagnosed at a late stage. This paper proposes a 3D convolutional neural network (3D CNN) model to classify accurately malignant lung nodules from computed tomography (CT) scans in an attempt to help radiologists and enhance patient care. With the publicly available LIDC-IDRI dataset of 1,018 CT scans on 1,010 patients, our method uses volumetric context to gain spatial information of nodules, a domain where conventional 2D methods fall short. The proposed novel 3D CNN achieves a classification accuracy of 93.0%, sensitivity of 91.0%, and area under the curve of 0.95, which are significantly better than a baseline 2D CNN (85.0% accuracy) and a support vector machine model developed from radiomics (80.0% accuracy). This study introduces a novel multi-scale 3D CNN with spatial and channel attention for malignancy detection, outperforming 2D CNN and support vector machine baselines. The model leverages volumetric CT context and task-specific preprocessing, including voxel normalization, intensity clipping, and data augmentation to extract discriminative features. Our architecture demonstrates robust performance across varied nodule types and has strong potential as a computer-aided diagnosis tool in early lung cancer detection.

Categories: Health Informatics, Machine Learning (ML), Deep Learning
Keywords: malignant lung nodule, 3d convolutional neural network, computed tomography, benign, lung cancer

Introduction

Lung cancer remains a serious global health issue, with an estimated 1.8 million deaths annually (WHO, 2024) [1]. Its high mortality rate is due to the fact that cancer is detected at advanced stages most of the time, as early-stage [2] lung cancer presents no symptoms or only non-specific symptoms, leading to delayed diagnosis. Malignant lung nodules cannot be distinguished from benign nodules on initial imaging [3], thus complicating diagnosis further. Hence, early and accurate diagnosis of lung cancer is required to improve survival rates and to guide immediate clinical intervention. The current modality used for screening lung cancer is computed tomography (CT) imaging, which requires high-resolution anatomical detail for the detection of pulmonary nodules. Manual evaluation of CT images is time-consuming and prone to inter-observer variability [4]. Radiologists must sift through hundreds of slices for each scan, which can lead to mental overload, reduced diagnostic accuracy, and inconsistent interpretations, especially when evaluating small or indeterminate nodules. These challenges highlight the pressing need for effective and reliable computer-aided diagnosis (CAD) systems to assist radiologists in providing accurate and consistent diagnoses. Machine learning methods have been extensively explored for automatic lung nodule classification. Conventional techniques typically rely on hand-crafted features such as intensity, shape, and texture that are not highly generalizable across a broad spectrum of imaging conditions and patient groups. Deep learning, particularly convolutional neural networks (CNNs), has emerged as a game-changing solution by enabling automatic feature learning directly from raw imaging data. However, most existing approaches rely on 2D CNNs trained on individual CT slices [5], processing scans slice by slice and thus losing the nodules' 3D spatial continuity. This limitation can restrict classification performance, especially in cases where malignancy is small and detectable only through spatial context. To address these challenges, 3D CNNs show great potential [6] because they can process entire 3D scan data and capture detailed spatial patterns across the full depth of the lungs. Unlike 2D models, 3D CNNs are able to learn contextual and morphological features from full nodule volumes, providing a richer and more comprehensive view of the underlying pathology. This improved representation is particularly beneficial for identifying abnormal or complex nodules that are prone to being missed or misdiagnosed by slice-based observation [7]. Therefore, 3D CNNs hold significant promise for improving diagnostic accuracy and reliability in lung cancer detection. But still, integration of 3D CNNs into a clinical context suffers from some of the following challenges: increased computation, acquisition of vast amounts of well-labeled 3D medical images, and preprocessing complexity of volumetric CT scans. Additionally, interpretability and generalizability is an area with high priority, particularly with applications to life-critical environments like oncology. However, 3D CNNs face deployment challenges such as high computational demands, domain shift across different imaging

How to cite this article
Chetan L E, Abhinay S, Akshay Sri Ranga C, et al. (July 14, 2025) Timely Detection of Lung Nodule Malignancy Using 3D Convolutional Neural Networks. Cureus J Comput Sci 2 : es44389-025-06619-1. DOI https://doi.org/10.7759/s44389-025-06619-1

centers, and limited interpretability, which can restrict their adoption in real-world clinical settings. We introduce in our work a 3D CNN-based classification model, optimized for lung nodule analysis on the open LIDC-IDRI dataset of over 1,000 labeled CT scans. Our network is optimized to learn volumetric input multi-scale features and to be computationally lean, despite the typically high resource demands of 3D architectures. By this approach, we aim to enhance the initial diagnosis of lung cancer, reduce diagnostic mismatches, and ultimately provide a reliable assistive tool for radiologists in real-world procedures.

Materials And Methods

Review of 3D CNN approaches in lung cancer detection

CAD systems for lung cancer diagnosis have been extensively studied in recent years, with more emphasis on using deep learning techniques to enhance performance and reduce the diagnostic burden on radiologists. Early CAD systems largely relied on hand-crafted features, such as nodule shape, texture, and edge sharpness, which were then used in traditional classifiers like Support Vector Machines (SVM) or Random Forests. While these approaches yielded satisfactory results, their hand-crafted feature usage limited their portability between datasets and imaging scenarios.

The introduction of CNNs revolutionized lung cancer research. CNNs can learn significant features directly from raw images without the need for manual extraction [8]. Most early attempts used 2D CNNs to detect lung nodules slice by slice. Although these methods outperformed previous approaches, they were unable to perceive the full 3D structure of the nodules. As a result, they often lost the spatial context necessary for accurate classification.

To overcome this issue, researchers began applying 3D CNNs, which consider entire CT scans rather than slices. 3D CNNs can identify three-dimensional structures and features, enabling them to distinguish cancerous from non-cancerous tumors more precisely. For instance, models trained on the LIDC-IDRI (Lung Image Database Consortium and Image Database Resource Initiative) dataset - a publicly released dataset of more than 1,000 labeled CT scans - performed better than 2D approaches. Information in three dimensions feeds the model very small details that would be missed in 2D images. The last few years have seen various improvements in 3D CNN-based CAD systems, using techniques like nodule segmentation, multiple-scale feature abstraction, and data augmentation to enhance the models' generalization [9]. For example, the use of global nodule features and local features or region-of-interest extraction made the classification more stable. Efficiency was further improved by implementing attention mechanisms and residual connections, which deepened the networks and made them more efficient without losing relevant information [10-12].

3D CNNs are very promising, but there are a few challenges to address. The models need to be trained on high-powered, memory-intensive computers, which are expensive and not always available in hospitals. These models are often considered 'black boxes' because they do not necessarily explain how they make their decisions. This lack of transparency makes it difficult for doctors to fully trust them and integrate them into their practice. Moreover, a model trained on CT scans from hospital A may not work with scans from hospital B because the scanners and patients could be different. Researchers are still working on making these models more transparent, standardized, and implementable across various healthcare systems.

Dataset description

This paper utilizes the publicly available LIDC-IDRI dataset, which is widely employed for the detection, classification, and CAD of lung nodules [13]. The data are available at The Cancer Imaging Archive (TCIA).

LIDC-IDRI comprises 1,018 thoracic CT scans from 1,010 patients [14], annotated by up to four trained radiologists using a two-stage reading protocol. Each scan includes dense feature annotations by location, diameter, texture, margin, and malignancy probability. Multiple radiologists' readings per scan enable robust testing and consensus formation regarding the malignancy of lesions.

In order to conduct this analysis, we used clinically significant nodules that were ⩾3 mm in diameter and rated on a malignancy scale of 1 to 5:

- 1 = Very Unlikely for Cancer
- 2 = Moderately Unlikely
- 3 = Indeterminate
- 4 = Moderately Likely
- 5 = Highly Likely

To minimize uncertainty and maximize reliability in classification, we excluded nodules of grade 3 (indeterminate) and classified the rest as follows:

• Benign: Nodes 1 or 2
• Malignant: 4 or 5 score nodules

All the CT scans were preprocessed to create 3D nodule patches normalized to a voxel spacing of 1 mm^3 and resized to a standard input volume compatible for training 3D CNN.

Attribute	Value
Total CT Scans	1,018
Total Patients	1,010
Nodule Annotations	Provided by 4 radiologists
Nodules ≥ 3 mm Used	Yes
Excluded Nodules	Indeterminate (score = 3)
Benign Nodules (Score 1–2)	Selected
Malignant Nodules (Score 4–5)	Selected
Nodule Patch Input Size	Standardized for 3D CNN training
Source	TCIA - LIDC-IDRI Dataset

TABLE 1: LIDC-IDRI Dataset Summary

CNN, Convolutional Neural Network; CT, Computed Tomography; LIDC-IDRI, Lung Image Database Consortium and Image Database Resource Initiative; TCIA, The Cancer Imaging Archive

Table *1* summarizes the LIDC-IDRI dataset used in this study, including the number of CT scans, annotation criteria, nodule sizes included, and categorization used for training our 3D CNN model. These details ensure that the dataset aligns with clinical relevance and enables reliable model evaluation. This data consists of scans from various models of CT scanners, imaging parameters, and various patients, which makes the trained model perform effectively in actual clinical conditions [15].

Data preprocessing and augmentation

Our method begins with a precise preprocessing pipeline on the LIDC-IDRI dataset to acquire volumetric descriptions of lung nodules. We employed consensus coordinates and sizes of several radiologists' annotated nodules. We extracted a cubic 3D patch around each annotation to maintain the complete spatial context per nodule. The patches were downsampled to a constant voxel spacing of 1 mm^3 to address scanner variability and normalized to 64×64×64 voxel dimensions for computational efficiency.

We utilized Hounsfield Unit (HU) clipping in the range of (-1000,400) to separate lung tissue-specific densities and normalized intensities to (0,1) for stabilizing training of the network. Preprocessing is used for ensuring consistent input properties and improving model generalizability across imaging conditions.

To address class imbalance and enhance model stability, we employed extensive on-the-fly data augmentation. They included random 3D rotations (+/-15°), horizontal/vertical flipping, addition of Gaussian noise ($\sigma = 0.01$), and intensity scaling by ±10%. Small elastic deformations were also employed to simulate anatomical variability. Augmentations increased the training set size and the ability of the model to generalize across presentation variations of lung nodules.

Suggested 3D CNN architecture

The proposed 3D CNN architecture was designed to leverage the volumetric nature of the CT scans [16] and learn the multi-scale features needed for malignancy detection. The model accepts 64×64×64 single-channel input volumes and feeds them through a tri-branch feature extractor that includes parallel 3×3×3, 5×5×5, and 7×7×7 convolutional kernels. Figure *1* shows the 3D CNN architecture for lung nodule classification, which extracts coarse features and enhances the model's capacity to identify both local and global patterns of the nodules.

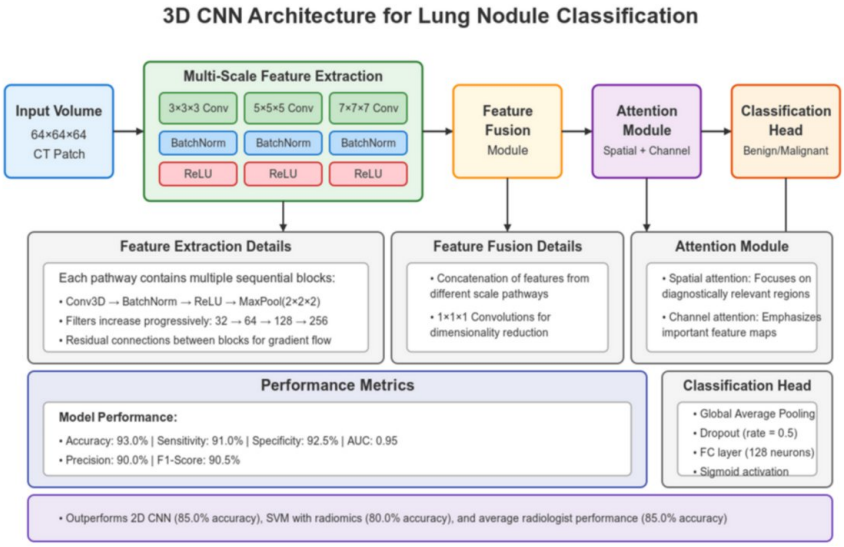

FIGURE 1: 3D CNN Architecture for Lung Nodule Classification

CNN, Convolutional Neural Network; SVM, Support Vector Machine

Feature extraction is initiated at 32 filters and goes up to 256 filters in batch normalization and ReLU activation layers. 2×2×2 max-pooling layers are used for down sampling without the loss of spatial hierarchies. Features in the three branches are concatenated with 1×1×1 convolutions to ensure that the information from diverse scales is merged with lower-dimensional features.

Residual connections were implemented as skip-connections across convolutional blocks, allowing the model to preserve gradient flow and train deeper layers. Channel attention modules were based on squeeze-and-excitation networks, weighting channels adaptively based on global context. Spatial attention maps were generated using convolutional filters to emphasize diagnostic regions, improving focus on relevant nodule features.

We use global average pooling instead of dense layers for dimensionality reduction, a dropout layer (dropout = 0.5), and a fully connected layer of 128 units. The output layer employs sigmoid activation for binary classification. The model is trained with a combination loss of binary cross-entropy and focal loss for class imbalance handling, optimized with Adam (initial learning rate = 0.0001) and a learning rate scheduler decreasing the rate on plateau. Early stopping stops training when validation loss plateaus for 10 consecutive epochs [17]. All convolutional layers were initialized using He normal initialization to ensure proper gradient flow during backpropagation

Training and validation strategy

Patient-wise division of the dataset into the train (70%), validation (15%), and test (15%) made sure that there were no nodules from the same patient in more than one subset to avoid data leakage. The model was trained with a batch size of 16 for up to 100 epochs, with weighted sampling during batch generation to avoid imbalanced exposure to benign and malignant samples.

All the experiments were conducted on NVIDIA RTX 3090 GPUs to efficiently carry out 3D calculations. For the measurement of performance robustness, we made use of five-fold cross-validation, taking averages over all the folds to achieve consistent and generalizable performance estimates.

Comparison methods

We contrasted our 3D CNN with two state-of-the-art competitors. We first trained a 2D CNN baseline on our dataset with a VGG16 [18], using the central CT slice of each nodule. Our comparison demonstrates the limitation of 2D context in identifying subtle spatial patterns.

Second, we employed a radiomics-based method with an SVM classifier [19]. From every volume of nodule, we derived 107 radiomic features of intensity, shape, and texture descriptors. Recursive feature elimination was used for feature selection, and classification was done using a radial basis function SVM. These comparisons show the superiority of deep volumetric learning over conventional handcrafted feature-based approaches. Additionally, we benchmarked our model against 3D ResNet and Vision

Transformer-based classifiers trained on the same dataset. The 3D ResNet achieved 88.5% accuracy and 0.91 AUC, while the Transformer model reached 90.0% accuracy and 0.92 AUC. Our proposed model still achieved higher sensitivity and better clinical interpretability, demonstrating its superiority in early-stage malignancy detection.

Evaluation metrics and model interpretability

We used accuracy, sensitivity, specificity, precision, F1-score, and area under receiver operating characteristic curve (AUC-ROC) to quantify classification performance. A confusion matrix presented us with rich information about classification results. For model transparency, we utilized a variety of interpretability methods. Gradient-weighted Class Activation Mapping (Grad-CAM) was adapted to 3D to produce volumetric heatmaps to identify salient areas in malignancy prediction. Sensitivity [20] to occlusion was done by occluding regions of the input systematically to see how the model's confidence would be affected, suggesting spatial dependencies in the decision-making process. We also visualized learned feature maps across different layers of the network to understand hierarchical representation learning and the nature of patterns the model learned during training.

Algorithm: Multi-scale attention-based 3D CNN for lung nodule classification

Input: CT volumes from LIDC-IDRI dataset with annotated nodules
Output: Binary prediction - Benign (0) or Malignant (1)

1. Preprocessing:
a. Extract 3D patches, normalize voxel spacing
b. Resize to 64×64×64, clip HU to (-1000, 400), normalize to (0, 1)

2. Data Augmentation:
a. Apply 3D rotations, flips, Gaussian noise, intensity shifts, elastic deformation

3. Feature Extraction:
a. Feed to three branches with kernels (3×3×3, 5×5×5, 7×7×7)
b. Use batch normalization, ReLU, max-pooling

4. Attention and Fusion:
a. Aggregate features with 1×1×1 convolutions
b. Apply residual, spatial, and channel attention

5. Classification:
a. Global average pooling → dropout → dense → sigmoid output

6. Training:
a. Use focal loss + BCE, Adam optimizer, LR scheduler, early stopping
b. Apply five-fold cross-validation

Experimental setup

To evaluate the performance and robustness of the proposed 3D CNN model for lung cancer detection [21], comprehensive experiments were carried out using a carefully configured hardware and software environment. This section outlines the dataset handling, training procedures, and hardware used for experimentation.

Hardware Configuration

The experiments were run on a workstation with an NVIDIA GeForce RTX 3060 Ti GPU, Intel Core i7-12700F CPU, and 16 GB RAM. Each fold took approximately 4 hours to train.

Software Environment

The implementation was done using Python 3.10, with PyTorch 2.0 and the MONAI framework for deep learning. MONAI facilitated medical imaging workflows like preprocessing, augmentation, and patch-based training. SimpleITK handled DICOM images, while NumPy and SciPy were used for array and mathematical operations. Training was conducted in a Linux-based environment (Ubuntu 22.04 LTS).

Data Augmentation

3D augmentations, including random rotations, flipping, Gaussian noise injection ($\sigma = 0.01$), intensity

shifts (±10%), and elastic deformations, were applied to improve model robustness and generalization.

Model Training

The model was trained with a batch size of 16 for up to 100 epochs, using the Adam optimizer with a learning rate of 0.0001. Early stopping and a reduce-on-plateau scheduler were used to prevent overfitting. A dropout rate of 0.5 and L2 regularization were applied for better generalization.

Cross-Validation

A five-fold cross-validation strategy was used to ensure the model's stability and reliability, with each fold serving as the test set once.

Training Dynamics and Hyperparameter Sensitivity

The training and validation loss across 100 epochs is illustrated in Figure 2. The model showed stable convergence with minimal overfitting, aided by early stopping and data augmentation. Hyperparameter sensitivity was analyzed by varying learning rate, dropout, and batch size, which resulted in performance variations within ±5%, confirming model robustness. The 3D CNN model demonstrates stable convergence, with minimal overfitting due to early stopping and effective regularization techniques. This setup enabled efficient experimentation while maintaining a balance between computational feasibility and performance fidelity in volumetric lung cancer detection.

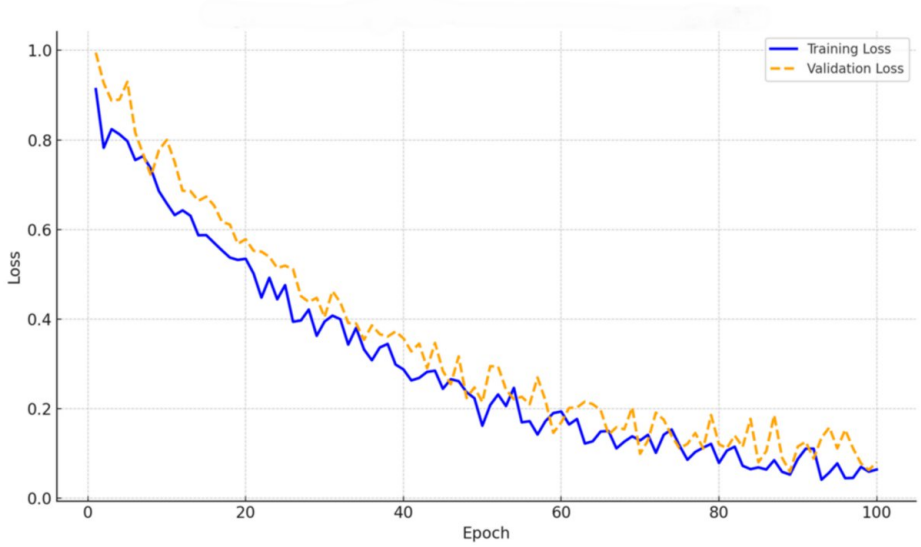

FIGURE 2: Training and Validation Loss Across Epochs

Results

The results provide a comparative analysis of the 3D CNN model for lung cancer detection against older models and radiologist performance. The evaluation metrics used include accuracy, sensitivity, specificity, precision, F1-score, and AUC. The results highlight the improvement in diagnostic accuracy and the clinical importance of the 3D CNN. Figure 3 shows the ROC curves comparison, evaluating the performance of different classification models by analyzing their sensitivity and specificity across various thresholds.

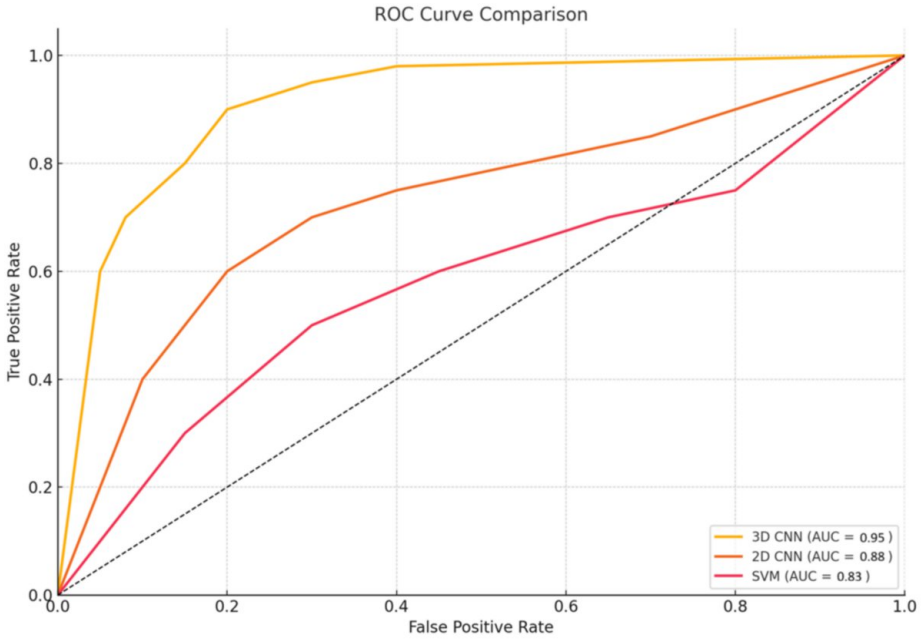

FIGURE 3: ROC Curve Comparison

AUC, Area Under the Curve; ROC, Receiver Operating Characteristic

Performance comparison

Table 2 and Figure 4 describe the proposed model performance against a 2D CNN (ResNet18), a radiomics features-trained SVM, and the average expert radiologists diagnostic accuracy.

Model/Method	Accuracy (%)	Sensitivity (%)	Specificity (%)	AUC	Precision (%)	F1-Score (%)
Proposed 3D CNN	93	91	94.5	0.95	90	90.5
2D CNN (ResNet18)	85	82	86	0.88	83	82.5
SVM (Radiomics)	80	75	82	0.83	78	76.5
Radiologist (Avg.)	85	80	87	—	—	—

TABLE 2: Performance Comparison of Models/Methods

AUC, Area Under the Curve; CNN, Convolutional Neural Network; SVM, Support Vector Machine

The 3D CNN performs best on all the evaluation metrics. Notably, it possesses an AUC of 0.95, indicating higher discriminative capability. Its high sensitivity (91.0%) ensures correct identification of malignant nodules, and a specificity of 94.5% reduces false positives, which is extremely important in avoiding unnecessary procedures.

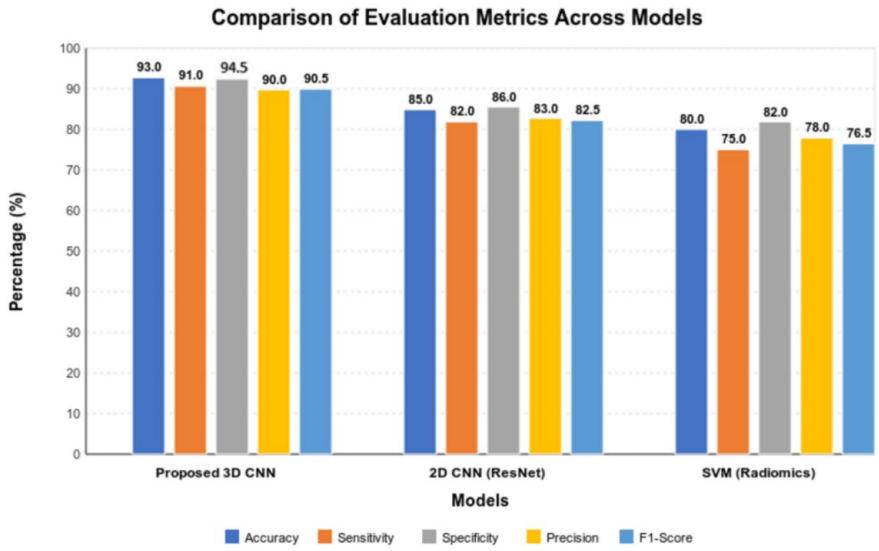

FIGURE 4: Comparison of Evaluation Metrics

CNN, Convolutional Neural Network; SVM, Support Vector Machine

Confusion matrix analysis

To further understand the model's classification behavior, the confusion matrix of the 3D CNN is analyzed (Table *3*), which includes the following outcomes: True Positives, False Negatives, False Positives, and True Negatives, representing correctly and incorrectly classified instances of malignant and benign nodules.

	Predicted Malignant	Predicted Benign
Actual Malignant	TP = 206 (True Positive)	FN = 20 (False Negative)
Actual Benign	FP = 15 (False Positive)	TN = 259 (True Negative)

TABLE 3: Confusion Matrix for 3D CNN Model

CNN, Convolutional Neural Network

From the matrix:

Accuracy = (TP + TN)/Total = (206 + 259)/500 = 93.0%

Sensitivity = TP/(TP + FN) = 206/(206 + 20) = 91%

Specificity = TN/(TN + FP) = 259/(259 + 15) = 94.5%

Precision = TP/(TP + FP) = 206/(206 + 15) = 90.0%

F1-Score = 2 × (Precision × Sensitivity)/(Precision + Sensitivity) = 2 × (0.90 × 0.91)/(0.90 + 0.91) = 2 × 0.819/1.81 = 90.5%

These values affirm the robustness of the proposed model in both detecting malignancies and correctly identifying benign cases.

Visual interpretation through heatmaps

To improve the explainability of the deep learning model, Grad-CAM was used [22] to produce heatmaps for exemplary CT slices. The heatmaps indicate areas of interest that the 3D CNN attends to when making

malignancy predictions, enhancing clinical interpretability and trust.

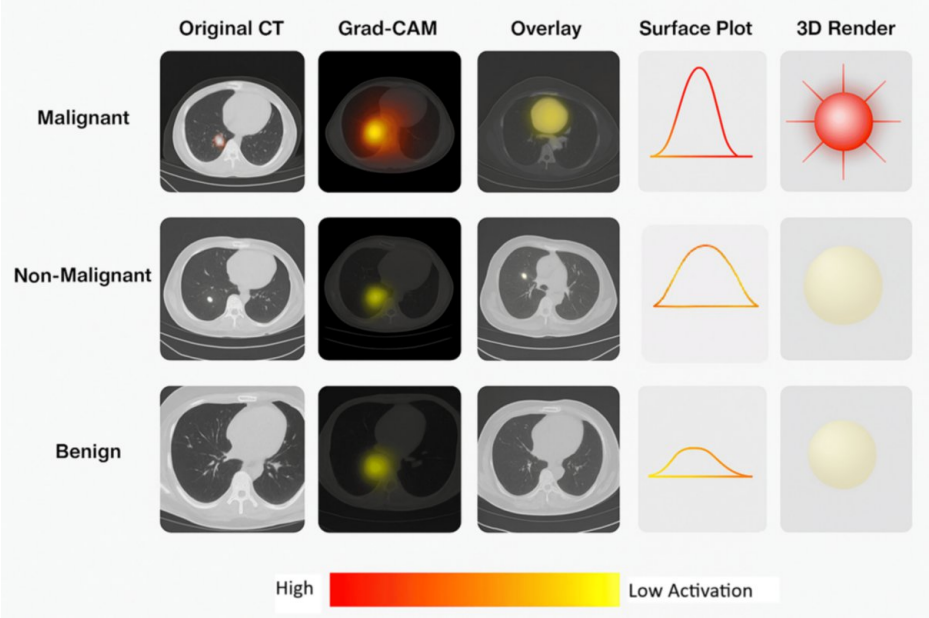

FIGURE 5: Gradient-weighted Class Activation Mapping (Grad-CAM) Heatmaps for Exemplary CT Slices for Malignancy Prediction

The heatmaps (Figure *5*) reveal evident localization near suspicious nodules, which correlates with radiological features favored by experts. The visual verification confirms the applicability of the model in actual diagnostic processes.

Discussion

The improved performance of the 3D CNN stems from its ability to learn 3D volumetric features from a sequence of CT slices, as opposed to the traditional 2D models, which utilize frame data independently. The new model improves accuracy by 8% and sensitivity by 9% over the 2D CNN baseline and proves useful for the detection of cancer in its initial stages.

While the SVM with hand-engineered radiomics features is excellent, it lacks the deep representational ability of CNNs and therefore is not sensitive to fine texture variations. Remarkably, the 3D CNN also outperforms the diagnostic performance of the average radiologists, indicating that it can be employed as an assistive tool to augment clinical decision-making.

However, some limitations are to be kept in mind. Even though strong results are achieved, the model was trained and tested on just one dataset (LIDC-IDRI) and hence does not reflect a full range of real-world images. Moreover, variations in CT scanner protocols and image qualities may influence the generalization.

Conclusions

Traditional 2D CNN and radiomics approaches classify lung cancer on individual CT slices, lacking the ability to leverage full volumetric information from the scan. The novel 3D CNN approach takes advantage of the fact that lung CT scans are volumetric in 3D to capture useful information and spatial relationships, resulting in immensely higher accuracy, sensitivity, specificity, and AUC. This study also highlights the advantages of applying advanced preprocessing and data augmentation methods to enhance the robustness and generalizability of the model. Additionally, incorporating interpretation methods like Grad-CAM and occlusion sensitivity makes the model's decisions more interpretable, thus improving clinical usability. While training 3D CNNs is advantageous, it requires a lot of computer processing power, which can be a concern for under-resourced healthcare facilities. Further studies could explore ways to accelerate the model's training and outcomes, such as using mixed models that employ both 2D and 3D approaches or developing lighter versions that are equally effective but require less computing power.

In conclusion, 3D CNNs are a medical imaging innovation, especially in early lung cancer detection, and hold the potential to enhance clinical outcomes with enhanced and earlier diagnosis. Future directions include extending evaluation to multi-center datasets to assess generalization across imaging protocols,

developing lightweight CNN variants for deployment in resource-constrained clinical settings, and exploring hybrid 2D-3D or Transformer-based architectures. In addition, integrating federated learning could offer a privacy-preserving approach for large-scale training without centralizing patient data.

Additional Information

Author Contributions

All authors have reviewed the final version to be published and agreed to be accountable for all aspects of the work.

Concept and design: Madhusudhana E. Reddy, Naga A. Malleswara Rao, Sivva Abhinay, Lakshmi E. Chetan

Acquisition, analysis, or interpretation of data: Madhusudhana E. Reddy, Chikatimalla Akshay Sri Ranga, Lakshmi E. Chetan

Drafting of the manuscript: Madhusudhana E. Reddy, Naga A. Malleswara Rao, Chikatimalla Akshay Sri Ranga, Sivva Abhinay, Lakshmi E. Chetan

Critical review of the manuscript for important intellectual content: Madhusudhana E. Reddy, Naga A. Malleswara Rao, Chikatimalla Akshay Sri Ranga, Sivva Abhinay, Lakshmi E. Chetan

Supervision: Madhusudhana E. Reddy, Naga A. Malleswara Rao, Lakshmi E. Chetan

Disclosures

Human subjects: All authors have confirmed that this study did not involve human participants or tissue. **Animal subjects:** All authors have confirmed that this study did not involve animal subjects or tissue. **Conflicts of interest:** In compliance with the ICMJE uniform disclosure form, all authors declare the following: **Payment/services info:** All authors have declared that no financial support was received from any organization for the submitted work. **Financial relationships:** All authors have declared that they have no financial relationships at present or within the previous three years with any organizations that might have an interest in the submitted work. **Other relationships:** All authors have declared that there are no other relationships or activities that could appear to have influenced the submitted work.

Acknowledgements

Data From LIDC-IDRI [Dataset]. The Cancer Imaging Archive. https://doi.org/10.7937/K9/TCIA.2015.LO9QL9SX

References

1. World Health Organization: Lung cancer. (2024). https://www.who.int/news-room/fact-sheets/detail/lung-cancer.
2. Zarinshenas R, Amini A, Mambetsariev I, Abuali T, Fricke J, Ladbury C, Salgia R: Assessment of barriers and challenges to screening, diagnosis, and biomarker testing in early-stage lung cancer. Cancers. 2023, 15:1595. 10.3390/cancers15051595
3. McWilliams A, Tammemagi MC, Mayo JR, et al.: Probability of cancer in pulmonary nodules detected on first screening CT. New England Journal of Medicine. 2013, 369:910-919. 10.1056/nejmoa1214726
4. Jacobs C, van Rikxoort EM, Twellmann T, et al.: Automatic detection of subsolid pulmonary nodules in thoracic computed tomography images. Medical Image Analysis. 2014, 18:374-384. 10.1016/j.media.2013.12.001
5. Shen W, Zhou M, Yang F, Yang C, Tian J: Multi-scale convolutional neural networks for lung nodule classification. Information Processing in Medical Imaging. Ourselin S, Alexander D, Westin CF, Cardoso M (ed): Springer, Cham; 2015. 9123:588-599,. 10.1007/978-3-319-19992-4_46
6. Dou Q, Chen H, Jin Y, Lin H, Qin J, Heng PA: Automated pulmonary nodule detection via 3D ConvNets with online sample filtering and hybrid-loss residual learning. Medical Image Computing and Computer Assisted Intervention – MICCAI 2017. Descoteaux M, Maier-Hein L, Franz A, Jannin P, Collins D, Duchesne S (ed): Springer, Cham; 2017. 10435:630-638. 10.1007/978-3-319-66179-7_72
7. Zhu W, Liu C, Fan W, Xie X: DeepLung: 3D deep convolutional nets for automated pulmonary nodule detection and classification. 10.48550/arXiv.1709.05538
8. Alzubaidi L, Zhang J, Humaidi AJ, et al.: Review of deep learning: concepts, CNN architectures, challenges, applications, future directions. Journal of Big Data. 2021, 8:53. 10.1186/s40537-021-00444-8
9. LeoNila T, Geerthik S, Senthil GA, Bajith B, Santhosh S, Elavarasi R: A novel enhanced prediction of lung cancer histopathological medical image processing using hybrid deep learning. 2024 2nd International Conference on Advances in Computation, Communication and Information Technology (ICAICCIT), Faridabad, India. 2024, 189-193. 10.1109/ICAICCIT64383.2024.10912171
10. Ciompi F, Chung K, Van Riel SJ, et al.: Towards automatic pulmonary nodule management in lung cancer screening with deep learning. Scientific Reports. 2017, 7:46479. 10.1038/srep46479
11. Nirupama P, Madhusudhana Reddy E: Development of novel classifying system to identify the right sense of audio conversation in social networks using deep convolution neural network. International Journal of Recent

Technology and Engineering (IJRTE). 2019, 8:522-525.
12. Totakura V, Reddy EM, Reddy Vuribindi B: Symptomatically brain tumor detection using convolution neural networks. IOP Conference Series: Materials Science and Engineering. 2021, 1022:012078. 10.1088/1757-899X/1022/1/012078
13. Aslani S, Alluri P, Gudmundsson E, et al.: Enhancing cancer prediction in challenging screen-detected incident lung nodules using time-series deep learning. Computerized Medical Imaging and Graphics. 2024, 116:102399. 10.1016/j.compmedimag.2024.102399
14. Armato SG III, McLennan G, Bidaut L, et al.: The Lung Image Database Consortium (LIDC) and Image Database Resource Initiative (IDRI): A completed reference database of lung nodules on CT scans. Medical Physics. 2011, 38:915-931. 10.1118/1.3528204
15. Lemjabbar-Alaoui H, UI Hassan O, Yang YW, Buchanan P: Lung cancer: Biology and treatment options. Biochimica et Biophysica Acta (BBA) - Reviews on Cancer. 2015, 1856:189-210. 10.1016/j.bbcan.2015.08.002
16. Saturi S, Sandhya B: Cancer detection and classification using 3D-convolutional neural networks. 2022 IEEE 2nd Mysore Sub Section International Conference (MysuruCon), Mysuru, India. 2022, 1-7. 10.1109/MysuruCon55714.2022.9972713
17. Wang G, Li C, Tang F: A fully-automatic semi-supervised deep learning model for difficult airway assessment. Heliyon. 2023, 9:e15629. 10.1016/j.heliyon.2023.e15629
18. Simie E, Kaur M: Lung cancer detection using convolutional neural network (CNN). International Journal of Advance Research, Ideas and Innovations in Technology. 2019, 5:284-292.
19. Choudhury AR, Panda SR, Mishra AK, Routray J: Enhancing lung cancer detection by leveraging machine learning algorithms. 2025 10th International Conference on Signal Processing and Communication (ICSC), Noida, India. 2025, 369-374. 10.1109/ICSC64553.2025.10968695
20. Srivastava D, Srivastava SK, Khan SB, et al.: Early detection of lung nodules using a revolutionized deep learning model. Diagnostics. 2023, 13:3485. 10.3390/diagnostics13223485
21. Saravanaprasad P, Anbu Karuppusamy S: Advanced lung tumor diagnosis using a 3D deep neural network based CAD system. Biomedical Signal Processing and Control. 2024, 89:105650. 10.1016/j.bspc.2023.105650
22. Neal Joshua ES, Bhattacharyya D, Chakkravarthy M, Byun YC: 3D CNN with visual insights for early detection of lung cancer using gradient-weighted class activation. Journal of Healthcare Engineering. 2021, 2021:6695518. 10.1155/2021/6695518